The Impact of Stratospheric Ozone Hole Recovery on Antarctic Climate

Judith Perlwitz,[1,2]

Steven Pawson,[3]

Ryan Fogt,[2]

J. Eric Nielsen, [3]

William Neff[2]

[1]Cooperative Institute for Research in Environmental Sciences

University of Colorado, Boulder, Colorado, USA

[2]NOAA Earth System Research Laboratory, Physical Sciences Division, Boulder, Colorado, USA

[3]Global Modeling and Assimilation Office, NASA Goddard Space Flight Center, Greenbelt, Maryland, USA

Abstract

Model experiments have revealed that stratospheric polar ozone depletion and anthropogenic increase of greenhouse gases (GHG) have both contributed to the observed increase of summertime tropospheric westerlies in the Southern Hemisphere (SH) with the ozone influence dominating. As the stratospheric halogen loading decreases in the future, ozone is expected to return to higher values, with the disappearance of the Antarctic ozone hole. The impact of this ozone recovery on SH climate is investigated using 21st century simulations with a chemistry climate model (CCM). The model response to the ozone recovery by 2100 shows that

tropospheric circulation changes during austral summer caused by ozone depletion between 1970 and 2000 almost reverse, despite increasing GHG concentrations. Comparison of the CCM results with multi-model scenario experiments from the Fourth Assessment Report (AR4) by the Intergovernmental Panel on Climate Change (IPCC) emphasize the importance of stratospheric ozone recovery for Antarctic climate.

Introduction

The SH polar climate has undergone significant changes over the past decades. The dominant change between 1969 and 1998 was the lower stratospheric cooling during austral spring [e.g.,*Thompson and Solomon,* 2002]. The accompanying dynamical response resulted in a one-month delay of the winter polar vortex breakdown with attendant consequences in the troposphere [*Neff,* 1999]. Tropospheric trends were characterized by a strengthening of the austral summer circumpolar westerlies, coincident with cooling over the Antarctic interior and warming over the Antarctic Peninsula [*Thompson and Solomon*, 2002]. These trends are consistent with a shift of the Southern Hemisphere Annular Mode (SAM) towards its positive phase. The hypothesis of *Thompson and Solomon* [2002] that these seasonal changes may be forced by lower stratospheric ozone loss has been verified in climate models [e.g., *Gillett and Thompson,* 2003]. Anthropogenic GHG increases also force the positive phase of the tropospheric SAM index [*e.g., Kushner et al.* 2001]. This affects the year-round circulation due to the increased meridional temperature gradient [*Brandefelt and Källén,* 2004]. The relative contributions of stratospheric ozone loss, GHG increases and natural forcings on recent tropospheric SAM trends have been widely studied. The consensus is that polar ozone changes are the biggest contributor to the observed tropospheric circulation changes during summer [e.g., *Shindell and Schmidt,* 2004*; Alblaster and Meehl*, 2006*; Miller et al.* 2006].

Surface observations show that human produced ozone-depleting substances (ODSs) are now declining and there are suggestions that the ozone hole is no longer growing [*e.g. Yang et al.,* 2005]. Using a parametric model, *Newman et al.* [2006] showed that recovery of the Antarctic ozone hole to 1980 levels will occur around 2068, and the area will very slowly decline between 2001 and 2017. At the same time, GHG concentrations are expected to continue to

rise, causing stratospheric cooling that may delay the ozone recovery. The relative contributions of ozone hole recovery and GHG increases on the SH circulation changes during the 21st century (C21) are not well quantified. *Shindell and Schmidt* [2004] found that GHG forcing and prescribed ozone recovery forcing oppose each other, resulting in small SAM trends during the first half of the C21. AR4 multi-model scenario experiments suggest that increased C21 GHG concentrations dominate the projected changes, with little impact from ozone [*Miller et al.*, 2006*; Arblaster and Meehl,* 2006]. However, ozone change scenarios were not uniformly defined among AR4 models. Some models did not include any time-dependent ozone forcing, other models prescribed time-dependent ozone depletion and ozone recovery, while a third group of models specified ozone depletion to 2000 but then retained these depleted values through the C21.

The goal of this study is to estimate the impact of ozone recovery on SH polar climate using a coupled chemistry climate model (CCM). The CCM include global dynamics and radiation, with interactive stratospheric ozone chemistry, providing a realistic tool to simulate changes in the ozone layer and their coupling to climate change. We will contrast the impacts of polar ozone depletion in the 20th Century (C20) and recovery in the C21 on the circulation, and relate the results to those from AR4 C21 simulations.

Model experiments

For this study, we used the Goddard Earth Observing System Chemistry-Climate model (GEOS CCM) Version 1 [*Pawson et al.,* 2008]. It includes radiative coupling between predicted middle atmospheric ozone and other GHGs with the atmospheric circulation. Sea-surface temperature (SST), sea ice and various trace gas concentrations are specified at the lower boundary of the model. Aspects of stratospheric ozone-temperature coupling and the climatology of the SH polar vortex have been evaluated by *Stolarski et al*. [2006], *Eyring et al.* [2006] and *Pawson et al.* [2008]. The model captures the main aspects of the global coupling between ozone and temperature. As with other CCMs, the Antarctic vortex breaks down too late in the season. Other weaknesses of the GEOS CCM are too much year-to-year variability in the vortex structure, a high initial bias in total ozone and a warm bias in lower stratospheric temperature when there is no chlorine-induced ozone loss, which mean that Antarctic ozone loss and ozone-induced cooling are overestimated [*Pawson et al*., 2008].

We analyze two simulations of the recent past (P-1 and P-2) and three C21 simulations (C21-HSST, C21-CSST and C21Cl1960). The atmospheric and lower boundary forcings of these transient simulations are summarized in Table 1. Simulations P-1 and P-2, starting from different initial conditions, are forced with observed changes in SST and sea ice [HadISST: *Rayner et al.,* 2003], GHG concentrations and halogens. GHG concentrations in the C21 runs follow IPCC scenario A1b (medium, SRESA1B). In C21-HSST and C21-CSST, the halogens are prescribed according to the Ab scenario [*WMO/UNEP,* 2003], while in C21Cl1960, chlorine is fixed at 1960 values. SST and sea ice distribution for the C21 simulations are taken from single AR4 SRESA1b simulations with the coupled ocean-atmosphere models HadGEM1 (C21-HSST) and CCSM3.0 (C21-CSST, C21Cl1960). Run C21-HSST was included in the multi-model analysis

of *Eyring et al*. [2007].

Table 1: Time Period, SST data set, scenarios for halogens and GHGs for GEOS CCM experiments.

Experiment	Time Period	SST	Halogens	Greenhouse Gases
P-1	1950-2004	Had1SST	Observed	Observed
P-2	1951-2004	Had1SST	Observed	Observed
C21-HSST	1996-2099	HadGEM1	WMO Baseline scenario Ab	IPCC/GHG scenario A1b (medium)
C21-CSST	2000-2099	CCSM3.0	WMO Baseline scenario Ab	IPCC/GHG scenario A1b (medium)
C21Cl1960	2001-2099	CCSM3.0	Chlorine fixed at 1960 values	IPCC/GHG scenario A1b (medium), with chlorine fixed at 1960 values

Results from GEOS CCM

Figure 1 shows the time series of 70-hPa minimum zonal mean ozone mixing ratio (OMR-min) reached between 90^{o}S and 60^{o}S on any day in October . Around year 1960, OMR-min is about 2.7 ppmv. Stratospheric halogen increases cause the strong decline of OMR-min to less than 0.1 ppmv. Although 1980 is commonly used as a baseline against which ozone depletion and recovery are evaluated, some Antarctic ozone is lost as halogen emissions increase in the 1970s. In the GEOS simulations, about 10% of the total Antarctic ozone is lost between 1970 and 1980 [*Pawson et al.,* 2008, Fig. 14]. As the stratospheric halogen loading decreases through the C21, the Antarctic ozone hole recovers. By the end of the C21, OMR-min reaches 1970 values. In C21Cl1960, OMR-min varies around 2.8 ppmv.

Figure 2 compares SH climate change for 1969 to 1999 (period I) and 2006 to 2094 (period II). The change for each period is defined as the difference between 11-year means centered on 1999 and 1969 (Period I) and 2094 and 2006 (period II). Monthly changes in polar cap (90^{o}S to 64^{o}S) ozone and temperature, and in mid-latitude (70^{o}S and 50^{o}S) zonal-mean zonal wind are investigated. In addition, three-month overlapping changes in the SAM index based on the surface pressure difference between 65^{o}S and 40^{o}S [*Gong and Wang, 1999*] are shown.

The left (right) panels of Fig. 2 show the results for period I (II) based on the ensemble mean of simulations P-1 and P-2 (C21-HSST and C21-CSST). The results discussed are very similar for the two individual simulations. They are significant on the monthly time scale in the stratosphere (99% level) and on the seasonal time scale in the troposphere (95% level).

Between 1969 and 1999 in P-1 and P-2, ozone loss over the polar cap migrates down from near 10 hPa in August to near 200 hPa in November, with largest loss between 50 and 70 hPa during October (Fig. 2a). (Tropospheric ozone in GEOS CCM is represented by relaxation to

climatology, so no trends are expected.) Polar ozone loss forces lower stratospheric cooling in the polar cap (Fig. 2c), most pronounced at 100 hPa in December.

The polar cooling increases the meridional temperature gradient and causes westerly zonal wind anomalies in the stratosphere (Fig. 2e). Changes in tropospheric westerlies maximize during December and January, lagging the stratospheric zonal wind changes by one month. The SAM index increases by 1.7 during summer (Dec.-Feb. mean, Fig. 2g).

The seasonality of tropospheric and stratospheric polar climate changes during austral spring and summer simulated with GEOS CCM agrees well with observations [*Thompson and Solomon,* 2002] and model sensitivity studies that prescribe observed ozone depletion. The simulated summer trends in near-surface circulation are very similar to observations (red crosses, Fig. 2g) despite the high bias of ozone changes. The mechanisms linking tropospheric circulation changes to stratospheric polar ozone changes are not well understood [*Thompson et al.,* 2006]. Idealized models reveal that this sensitivity results from a complex feedback involving synoptic scale eddies in the troposphere, and is not purely a local response to the ozone induced temperature changes [*Kushner and Polvani,* 2004; *Song and Robinson*, 2004].

Projected changes for 2006-2094 (Fig. 2, right panels) are now contrasted with those for 1969-1999. Polar ozone depletion and recovery are clearly characterized by very similar seasonal changes with opposite signs. Because the ozone-hole recovery occurs more slowly than the onset (Fig. 1), these circulation changes occur over different periods (around 30 years for onset versus 90 years for recovery). The main features related to ozone recovery are the maximum ozone increase at 50 hPa during October (Fig. 2b), and subsequent warming (Fig. 2d) and weakening westerlies in the lower stratosphere (Fig. 2f). Main tropospheric changes linked to the seasonal impact of ozone recovery are the near 2 m/s decrease of the circumpolar westerlies during

summer. The Dec-Feb. mean SAM index decreases by 1.4 (Fig. 2h). Comparing the Dec-Feb. changes in SAM index in periods I (+1.7) and II (-1.4) suggests that changes caused by polar ozone depletion during 1969-1999 almost reverse during the C21 (Figure S1 in auxiliary material). Note that this change may be too large because of the high ozone bias in GEOS CCM when the halogen loading is low [*Pawson et al.,* 2008].

A comparison between the CCM runs that are forced with and without chlorine changes (Fig. 2, Fig. S2) clearly point out the seasonal (spring to summer) impact of ozone recovery in the changing atmosphere. GHG increases cause a year-round cooling of the stratosphere (Fig. S1b) and strengthening of the tropospheric westerlies (Fig. S2c, green lines in Figs. 2h and S2d).

Comparison with AR4 C21 simulations

The results from GEOS CCM motivate a re-examination of the impacts of ozone change in the C21 AR4 simulations. For comparison, two grand ensemble means (see Table S1 in the auxiliary material) of 21 and 19 multi-model AR4 SRESA1B simulations are investigated; these either include (AR4-O_3Rec) or exclude (AR4-O_3Const) ozone recovery. This analysis differs from that of *Miller et al.* [2006] because the ensemble AR4-O_3Rec excludes the simulations that fixed ozone at the suppressed 2000 values throughout the C21.

Figure 3 shows the seasonal cycle of three-month overlapping total changes in the SAM index during period II for the two AR4 grand ensembles and CCM simulations. In winter, AR4-O_3Const and AR4-O_3Rec both exhibit a significant increase of the SAM index due to increasing GHGs. Approaching austral summer the SAM index change remains positive in AR4-O_3Const, while in AR4-O_3Rec a distinct seasonality emerges as the SAM index change approaches zero.

The impact of the Antarctic ozone hole recovery on the summer circulation is more pronounced in the CCM simulations C21-HSST and C21-CSST, exhibiting a significant decrease of the SAM-index (Fig. 3). Fig. 3 also illustrates that the summertime increase in SAM index is similar between the simulation with fixed chlorine (C21Cl1960) and AR4-O_3Const meaning that increasing GHG concentrations have a similar impact on tropospheric summer circulation in the AR4 and GEOS CCM model configurations. During winter, when we expect the GHG influence to dominate, there is a wide spread between the individual GEOS CCM simulations: larger ensembles are needed to fully characterize differences between the CCM and AR4 models.

Conclusions

The impact of Antarctic ozone hole recovery on SH polar climate was investigated using the GEOS CCM. The ozone recovery through the C21 leads to a warming of the polar stratosphere during spring, weaker westerly zonal winds in the stratosphere during late spring and early summer and in the troposphere during summer. These seasonal changes reverse those caused by Antarctic ozone depletion in the late C20.

The main result concerns the combined impacts of stratospheric ozone recovery and GHG increases on the seasonal changes in the Antarctic tropospheric circulation. Prior studies have established that GHG increases cause a year-round positive shift of the SAM index. Excluding the onset and recovery of the ozone hole from GEOS CCM leads to a similar response. Runs C21-HSST and C21-CSST demonstrate that the Antarctic ozone hole recovery during the C21 has a seasonal effect on the SH tropospheric circulation that dominates and opposes the GHG-induced positive tendency of the SAM index. As a consequence, the C21 summertime SAM index decreases significantly.

Some comparisons were made with ensembles of AR4 simulations. Separation of the C21 simulations into two groups that do and do not represent ozone recovery revealed that the impact of ozone recovery is significant but smaller than in the GEOS CCM. The differences between the AR4 and CCM simulations most likely arise from the more complete representation of the middle atmosphere in the CCM, especially the interactive ozone forcing. There are several uncertainties to this conclusion:

- The GEOS CCM results were deduced from three simulations, compared to ensemble averages for the AR4 models. Although the causality of the changes in GEOS CCM is clear, the magnitude of the response may be reduced in an ensemble average.

- Because the GEOS CCM simulations omit the coupling to an interactive ocean model, the coupling among the middle atmosphere-troposphere-ocean/sea ice was not represented.
- Other CCMs differ in features of stratospheric climatology (e.g., interannual variability of the polar vortex, final vortex breakup in spring) and coupling to the troposphere (e.g., vertical propagation of wave activity). They also give diverse predictions of the year when ozone recovers to pre-ozone-hole values [*Eyring et al*. 2007].
- The relative contributions of ozone recovery and GHG increases on tropospheric circulation will also be sensitive to the GHG scenario used in the simulations.

These points can be addressed in several ways. First, comparison of results from the various CCMs in *Eyring et al.* [2007] with AR4 simulations is underway and yields results consistent with those reported here (Son, Polvani, and Waugh, personal communication, 2008). Second, simulations with different GHG and ODS evolutions will be helpful for examining the changes in the late C21. Third, the climate responses to ozone change can be fully investigated in models that include coupling between ocean, atmosphere and chemistry.

These results of this study support the argument for including stratospheric processes in assessments of the impact of anthropogenic forcings on climate. The growth and decay of the ozone hole leads to a discernable signature on Antarctic surface climate change, which in summertime dominates the change induced by increased GHGs. This ozone-induced anomaly peaks near the time of maximum ozone depletion and decays over several decades, after which the GHG-induced change begins to dominate. The full climate impacts of ozone change will be more completely addressed using CCMs coupled to full-depth ocean and interactive sea ice modules, which should capture the inertia of the anomalous radiative forcing and the air-sea interactions arising from the slowdown of the tropospheric westerlies – these feedbacks could

modify the seasonality and the longevity of the response isolated in this study.

Acknowledgments. This work was supported by the NASA Modeling and Analysis Program and used high-end computational resources provided by NASA's Columbia Project. R. Fogt's contribution was supported by the National Research Council Research Associateship Programs. We thank L. Polvani and two reviewers for helpful comments on this manuscript. We acknowledge the modeling groups, the Program for Climate Model Diagnosis and Intercomparison (PCMDI) and the WCRP's Working Group on Coupled Modeling (WGCM) for their roles in making available the WCRP CMIP3 multi-model dataset. Support of this dataset is provided by the Office of Science, U.S. Department of Energy.

References:

Arblaster, J.M., and G.A. Meehl (2006), Contributions of external forcings to Southern Annular Mode trends, *J. Clim.*, *19*, 2896-2905.

Brandefelt, J. and E. Källén (2004), The response of the Southern Hemisphere atmospheric circulation to an enhanced greenhouse gas forcing, *J. Clim.*, *17*, 4425-4442.

Eyring, V., et al. (2006) Assessment of temperature, trace species and ozone in chemistry-climate model simulations of the recent past, *J. Geophys. Res.*, *111*, D22308, doi:10.1029/2006JD007327..

Eyring, V., et al. (2007), Multimodel projections of stratospheric ozone in the 21st century, *J. Geophys. Res.*, *112*, D16303, doi:10.1029/2006JD008332.

Gillett, N., and D. W. J. Thompson (2003), Simulation of recent Southern Hemisphere climate change, *Science*, *302*, 273-275.

Gong, D., and S. Wang (1999), Definition of Antarctic oscillation index, *Geophys. Res. Lett.*, *26*, 459–462.

Kushner, P. J., I. M. Held, and T. L. Delworth (2001), Southern Hemisphere atmospheric circulation response to global warming, *J. Clim.*, *14*, 2238–2249.

Kushner, P. J. and L.M. Polvani (2004), Stratosphere-troposphere coupling in a relatively simple AGCM: The role of eddies, *J. Clim.*, *17*, 629-639.

Marshall, G. J. (2003), Trends in the Southern Annular Mode from observations and reanalyses, *J. Clim.*, *16*, 4134–4143.

Miller, R.L., G.A. Schmidt, and D.T. Shindell (2006), Forced annular variations in the 20th century Intergovernmental Panel on Climate Change Fourth Assessment Report models. *J. Geophys. Res.*, *111*, D18101, doi:10.1029/2005JD006323.

Neff, W. D. (1999), Decadal time scale trends and variability in the tropospheric circulation over the South Pole, *J. Geophys. Res., 104,* 27217-27251.

Newman, P. A., E. R. Nash, S. R. Kawa, S. A. Montzka, and S. M. Schauffler (2006), When will the Antarctic ozone hole recover?, *Geophys. Res. Lett., 33*, L12814, doi:10.1029/2005GL025232.

Pawson, S., R. S. Stolarski, A. R. Douglass, P. A. Newman, J. E. Nielsen, S. F. Frith, and M. K. Gupta (2008), Goddard Earth Observing System Chemistry-Climate Model Simulations of Stratospheric Ozone-Temperature Coupling between 1950 and 2005, *J. Geophys. Res.,* in press.

Rayner, N. A., D. E. Parker, E. B. Horton et al. (2003), Global analyses of sea surface temperature, sea ice, and night marine air temperature since the late nineteenth century, *J. Geophys. Res., 108*(D14*),* 4407, doi:10.1029/2002JD002670.

Shindell, D.T., and G.A. Schmidt, (2004), Southern Hemisphere climate response to ozone changes and greenhouse gas increases. *Geophys. Res. Lett., 31*, L18209, doi:10.1029/2004GL020724.

Song, Y., and W. A. Robinson, (2004): Dynamical mechanisms for stratospheric influences on the troposphere, *J. Atmos. Sci., 61*, 1711-1725.

Stolarski, R. S., A. R. Douglass, M. Gupta, P. A. Newman, S. Pawson, M. R. Schoeberl, and J. E. Nielsen (2006), An ozone increase in the Antarctic summer stratosphere: A dynamical response to the ozone hole, *Geophys. Res. Lett., 33*, L21805, doi:10.1029/2006GL026820.

Thompson, D. W. J. and S. Solomon (2002), Interpretation of Recent Southern Hemisphere Climate Change, *Science, 296,* 895-899.

Thompson, D.W.J., J.C. Furtado, and T.G. Shepherd, (2006), On the Tropospheric Response to Anomalous Stratospheric Wave Drag and Radiative Heating. *J. Atmos. Sci., 63*, 2616-2629.

World Meteorological Organization/United Nations Environment Programme (WMO/UNEP) (2003), Scientific Assessment of Ozone Depletion: 2002, *Rep. 47*, World Meteorol. Org., Global Ozone Res. and Monit. Proj., Geneva, Switzerland.

Yang, E.-S., D. M. Cunnold, M. J. Newchurch, and R. J. Salawitch (2005), Change in ozone trends at southern high latitudes, *Geophys. Res. Lett.*, *32*, L12812, doi:10.1029/2004GL022296.

J. Perlwitz, R. Fogt and W. Neff, Physical Sciences Division, NOAA Earth System Research Laboratory, 325 Broadway, Boulder CO 80305-3337, USA. (judith.perlwitz@noaa.gov)

S. Pawson, and J. E. Nielsen, Global Modeling and Assimilation Office, NASA Goddard Space Flight Center, Code 610.1, Greenbelt, MD 20771, USA.

Figure Captions

Figure 1:

Time series of 70-hPa minimum zonal mean ozone mixing ratio [ppmv] over SH polar cap area (between 90^{o}S and 60^{o}S) during October (using daily model output).

Figure 2:

Monthly changes in polar cap ozone (90^{o}S-64^{o}S), polar cap temperature (90^{o}S-64^{o}S), mid-latitude zonal wind (70^{o}S-50^{o}S), and 3-month overlapping changes of near surface SAM index (blue lines in Fig2.g and h). Left panels: period I (ensemble mean [P-1,P-2]), right panels; period II (ensemble mean [C21-HSST,C21-CSST]). Red crosses in Fig.2g indicates observed changes in SAM index based on Marshall index [*Marshall, 2003*]. Green line in Fig. 2h indicates values for C21Cl1960. Labels in Fig. 2g and 2h indicate center month of 3-month mean.

Figure 3:

Time series of three month overlapping changes of near surface SAM determined as surface pressure difference between 40^{o}S and 65^{o}S for period II for AR4-O_3Rec (dashed black line: 21-member ensemble mean; grey shading: 95% confidence interval), AR4-O_3Const (solid black line: 19-member ensemble mean; brown shading: 95% confidence interval) and GEOS CCM (blue star symbol: C21-HSST; blue plus symbol: C21-CSST, solid blue line: mean [C21-HSST, C21-CSST]; solid green line: C21Cl1960).

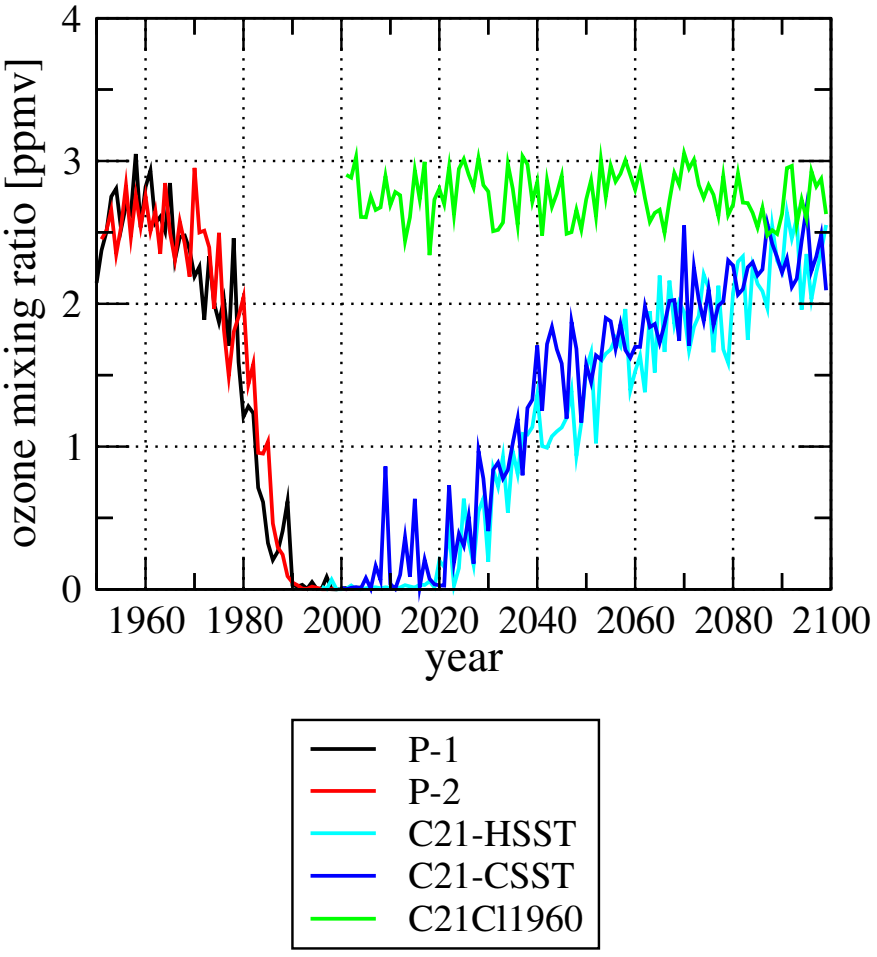
ozone mixing ratio [ppmv]
4
3
2
1
0
1960
1980
2000
2020
2040
2060
2080
2100
year
P-1
P-2
C21-HSST
C21-CSST
C21Cl1960

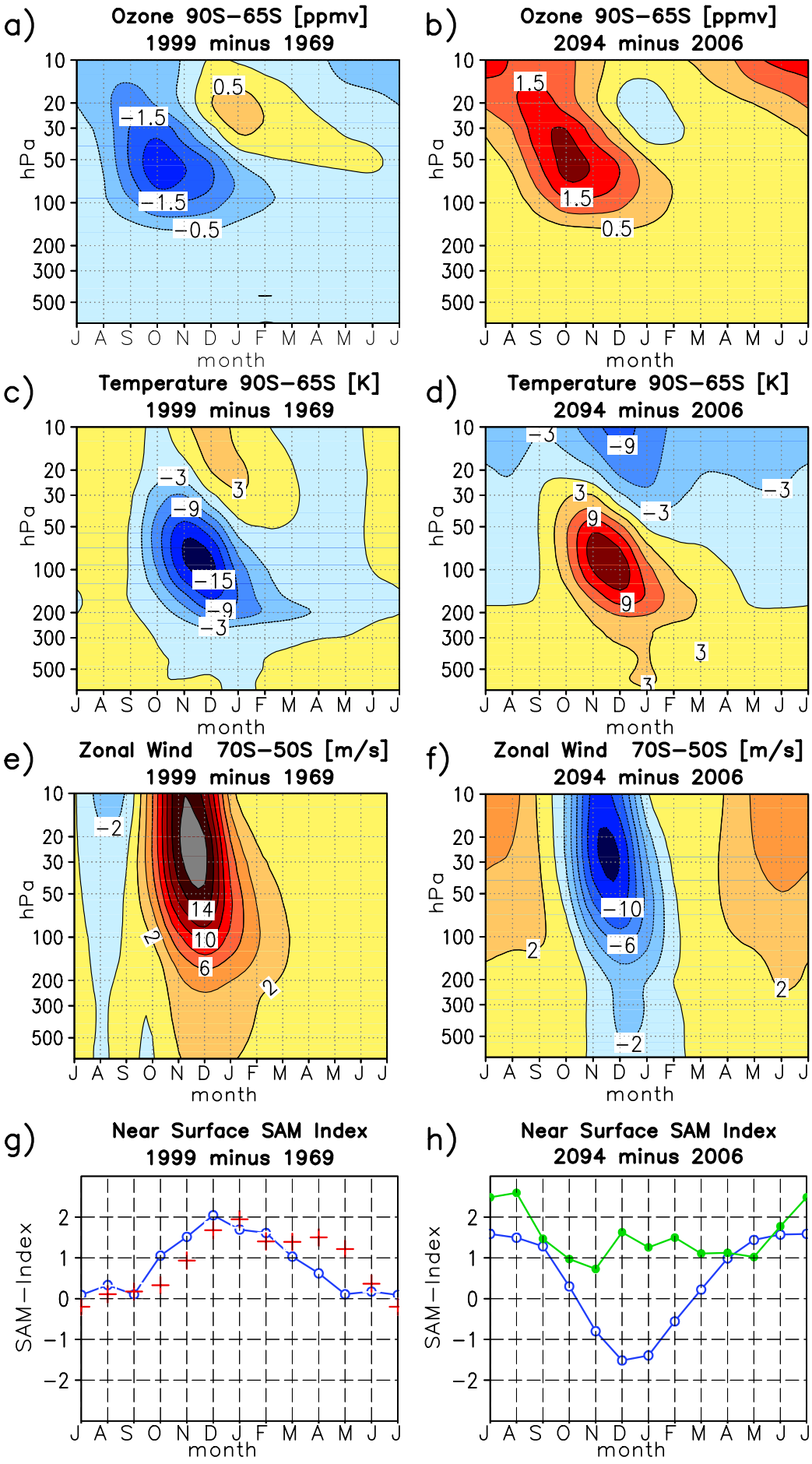
a)
Ozone 90S–65S [ppmv]
1999 minus 1969
b)
Ozone 90S–65S [ppmv]
2094 minus 2006
c)
Temperature 90S–65S [K]
1999 minus 1969
d)
Temperature 90S–65S [K]
2094 minus 2006
e)
Zonal Wind 70S–50S [m/s]
1999 minus 1969
f)
Zonal Wind 70S–50S [m/s]
2094 minus 2006
g)
Near Surface SAM Index
1999 minus 1969
h)
Near Surface SAM Index
2094 minus 2006
hPa
month
SAM–Index
J A S O N D J F M A M J J

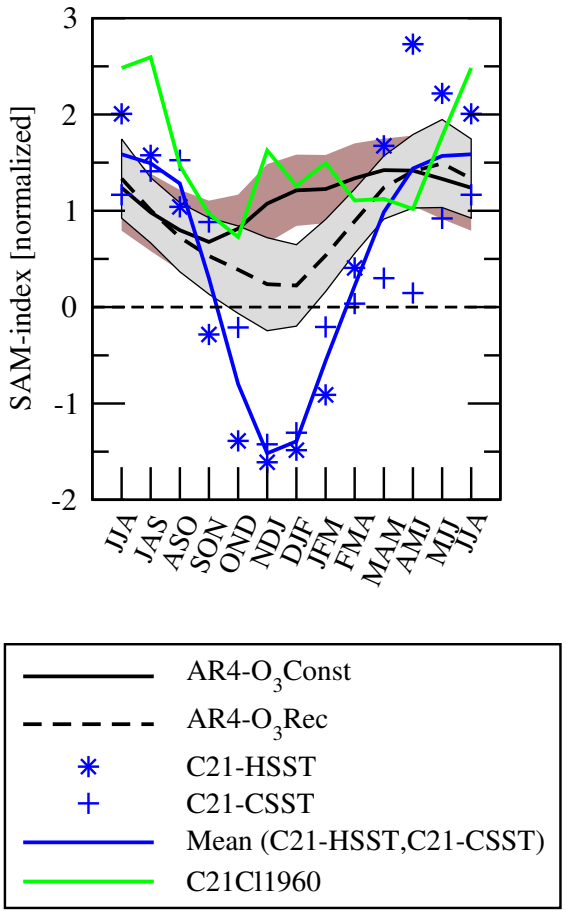
SAM-index [normalized]
3
2
1
0
-1
-2
JJA
JAS
ASO
SON
OND
NDJ
DJF
JFM
FMA
MAM
AMJ
MJJ
JJA
AR4-O3Const
AR4-O3Rec
C21-HSST
C21-CSST
Mean (C21-HSST,C21-CSST)
C21Cl1960

Auxiliary Material:

Table S1. Description of the IPCC AR4 general circulation models used in the study. Members = number of ensemble runs used for A1b scenarios, ozone = indication of whether or not model contains ozone recovery forcing; horizontal resolution = approximate output resolution of models; model top = height of atmospheric model top.

Model	Country	SRES A1B Members	Ozone	Horizontal Resolution (lon x lat, degrees)	Vertical Levels	Model Top (hPa)
CCCMA[a] CGCM3.1	Canada	5	N	2.80 x 2.80	31	1
IAP[c] FGOALS	China	3	N	2.81 x 2.81	26	2.2
IPSL [d] CM4	France	1	N	3.75 x 2.50	19	4
MIROC[e] MedRes	Japan	3	Y	2.81 x 2.81	20	30 (km)
MIUB[f] ECHO_G	Germany / Korea	3	N	3.90 x 3.90	19	10
MPI [g] ECHAM5	Germany	3	Y	1.88 x 1.88	31	10
MRI [h] CGCM2	Japan	5	N	2.81 x 2.81	30	0.4
NASA GISS[i] Russell AOGCM	USA	2	N	4.00 x 3.00	12	10
NCAR [j] CCSM3.0	USA	7	Y	1.41 x 1.41	26	2.2
NCAR PCM1	USA	4	Y	2.81 x 2.81	18	2.2
NOAA GFDL[k] CM2.0	USA	1	Y	2.50 x 2.00	24	3
NOAA GFDL CM2.1	USA	1	Y	2.50 x 2.00	24	3
UKMO [l] HadCM3	UK	1	Y	3.75 x 2.50	19	5
UKMO HadGEM1	UK	1	Y	1.875 x 1.25	38	39.2 (km)

[a]Canadian Centre for Climate Modelling and Analysis
[c]Institute of Atmospheric Physics
[d]Institut Pierre Simon Laplace
[e]Model for Interdisciplinary Research on Climate
[f]Meteorological Institute of the University of Bonn
[g]Max Planck Institute for Meteorology
[h]Meteorological Research Institute
[i]National Aeronautics and Space Administration Goddard Institute for Space Studies
[j]National Center for Atmospheric Research
[k]National Oceanic and Atmospheric Administration Geophysical Fluid Dynamics Laboratory
[l]United Kingdom Meteorological Office, Hadley Centre

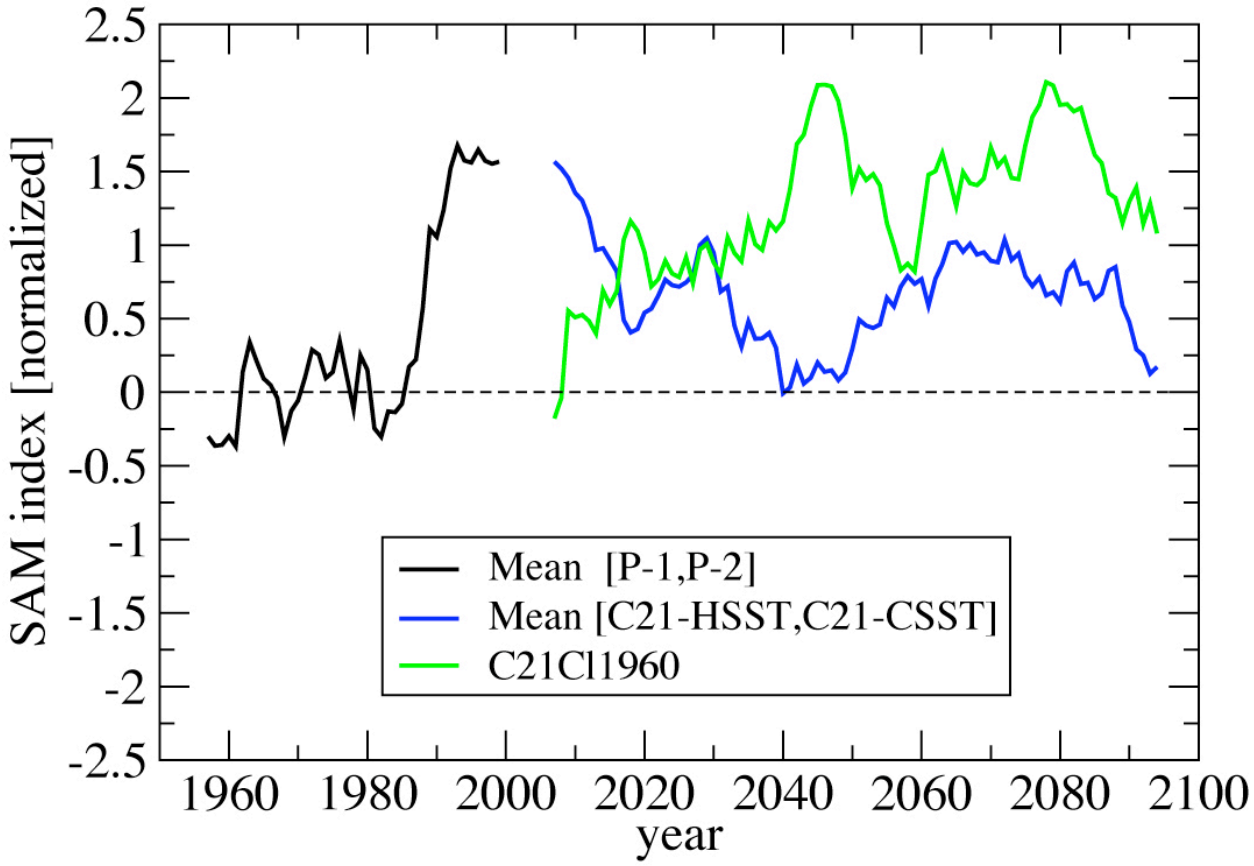

Figure S1:
The smoothed time series (11-year running average) of normalized summertime (Dec.-Feb.) SAM index for the mean [P-1,P-2] (black line), the mean [C21-HSST ,C21-CSST] (blue line), and for the C21Cl1960 run (green line).

1

2

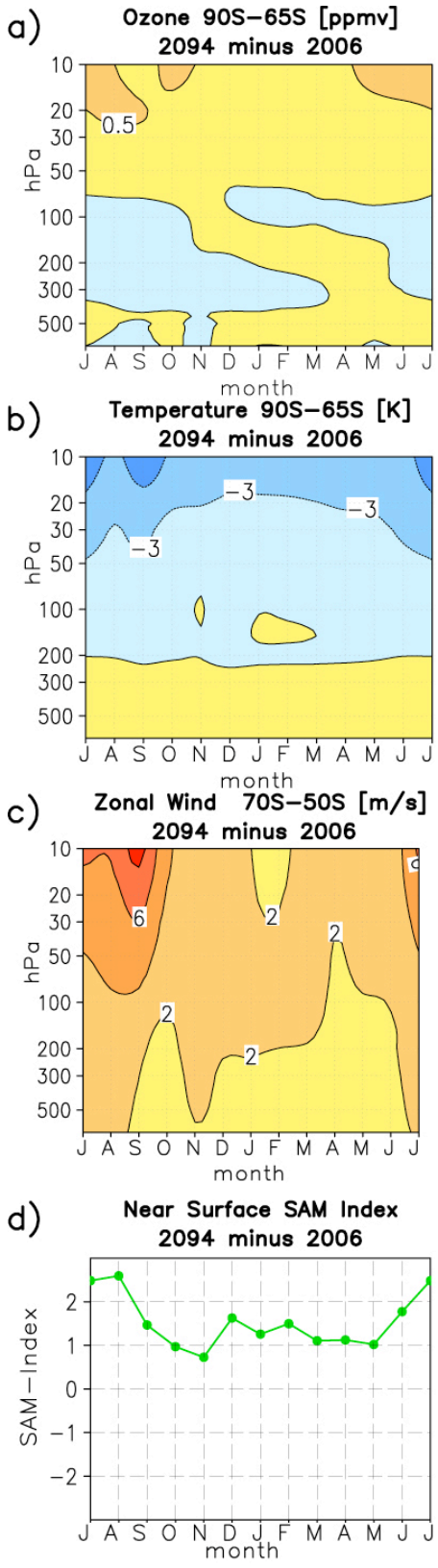

Figure S2: Monthly changes in polar cap ozone (90°S-64°S), polar cap temperature (90°S-64°S), mid-latitude zonal wind (70°S-50°S), and 3-month overlapping changes of near surface SAM index for C21Cl1960.